RSC Advances

ROYAL SOCIETY OF CHEMISTRY

www.rsc.org/advances

Extended Structural Materials Composed of Transition-Metal-Substituted Arsenicniobates and Their Photocatalytic Activity

Qing Lan,[a] Zhi-Ming Zhang,*[a] Yang-Guang Li,[a] and En-Bo Wang*[a]

[a]*Key laboratory of Polyoxometalate Science of Ministry of Education, Department of Chemistry, Northeast Normal University, Renmin Street No.5268, Changchun, Jilin, 130024, P. R. China.*

E-mail: zhangzm178@nenu.edu.cn (Z. M. Zhang), wangeb889@nenu.edu.cn (*E. B. Wang*)

Abstract

Two novel transition-metal-cluster-containing arsenicniobates, $[Cu(en)_2(H_2O)][Cu(en)_2]_4\{AsNb_9V_7O_{44}\}\cdot 8H_2O$ **(1)** and $[Cu(en)_2(H_2O)][Cu(en)_2]_4H\{AsNb_8V_8O_{44}\}\cdot 11H_2O$ **(2)**, were designed and synthesized by reaction of $K_7HNb_6O_{19}\cdot 13H_2O$, $Cu(Ac)_2\cdot H_2O$, Na_2VO_3, As_2O_3, and en molecules. Structural analysis revealed that compounds **1** and **2** contained the structural similar $[AsNb_9V_7O_{44}]^{10-}$ and $[AsNb_8V_8O_{44}]^{11-}$ polyoxoanions, respectively, which are obtained by inserting a $\{NbV_7\}$ or $\{V_8\}$ ring into the tetravacant polyoxoniobate $[AsNb_8O_{36}]^{27-}$. Polyoxoanions in **1** and **2** could be regarded as the Keggin polyoxoniobates $[AsNb_9V_3O_{40}]$ or $[AsNb_8V_4O_{40}]$ capped by four VO_5 units. The high-nuclear vanadium clusters were firstly introduced into the Keggin-type arsenicniobates. Further, polyoxoanions in **1** and **2** were connected by the metal-organic linkers into the 1D chain and 2D layer-like framework, respectively. Photocatalytic studies indicated that compounds **1** and **2** are both active for photocatalytic degradation of organic dye in aqueous solution, and they are stable and easily separated from the photocatalytic system for reuse as well.

Introduction

Polyoxometalates (POMs) are an outstanding class of nanosized metal-oxo clusters with wide structural diversity and O-enriched surfaces. They have received much attention as their fascinating properties and potential applications in many different fields.[1] Among the POM family, polyoxotungstates, polyoxomolybdates, and polyoxovanadates are the dominant subclasses as they can be easily synthesized by simple acidification and exist with a wide pH range.[2,3] Polyoxoniobates (PONs) attracted more and more attention recently as they possess of potential applications in various fields such as photocatalysis, nuclear-waste treatment, and base-catalyzed decomposition of biocontaminants.[4] To date, many isopolyoxoniobates, such as $[Nb_6O_{19}]^{8-}$ and $[Nb_{10}O_{28}]^{6-}$, $[Nb_{20}O_{54}]^{8-}$, $[H_9Nb_{24}O_{72}]^{15-}$, $[HNb_{27}O_{76}]^{16-}$, $[Nb_{32}O_{96}H_{28}]^{4-}$, and their transition-metal Ti-, Cr-, V- and Cu- containing derivatives were synthesized.[5-7] Compared to the isopolyoxoniobate chemistry, the development of heteropolyniobate (HPON) is still in its infancy stage. In 2002, the first HPON $\{[Ti_2O_2][SiNb_{12}O_{40}]\}^{12-}$, where the Keggin-type HPON was connected into an infinite one-dimensional (1D) chain, was reported by Nayman et al.[8] Inspired by this pioneering work, several Keggin-type HPONs, *C*-type HPONs and their derivations were prepared subsequently.[9] These HPON compounds were obtained by introducing Si, Ge and V into the HPON structure $[TNb_{12}O_{40}]$ (T = Si, Ge and V).[10] As well known, Keggin and Wells-Dawson-type POMs are the most widely recognized and thoroughly studied and, they have been widely used as the precursors and building units for constructing functional materials.[11,12] Introduction of novel heteroatom to the

typical POMs will not only increase the variety of POM chemistry, but also can supply new candidates for design and synthesis of function materials. Arsenic, located below the phosphorus and right the germanium in the periodic table of elements, has similar chemical properties or atomic radius with them.[13] The introduction of As into the HPONs provided a new type of the PON family, and a new candidates for design and synthesis of function materials. This will be a promising field for construction new PON compounds. Up to date, the research of arsenicniobate chemistry is still rarely explored.[14,15] We have long-term committed to the research of PONs, and a series of P, Ge, V and Si-centered PONs $[XNb_8V^{IV}_8O_{44}]$ (X = P and V), $[PNb_{12}O_{40}(VO)_6]$, $[GeNb_{12}V^{IV}_2O_{42}]$, $[SiNb_{12}V^{IV}_2O_{42}]$ were designed and synthesized.[16] Here, the arsenic atom as heteroatom was introduced to the PON structure resulting in two Keggin-type polyoxoanions $[AsNb_8V_4O_{40}]$ and $[AsNb_9V_3O_{40}]$ capped by four VO_4 units, which were further connected by $[Cu(en)_2]^{2+}$ metal-organic groups into the 1D chain and 2D layer-like framework, respectively. Photocatalytic studies indicate that compounds **1** and **2** are both active for photocatalytic degradation of organic dye in aqueous solution.

Experimental section

Materials and Methods. All chemicals were commercially purchased and used without further purification. $K_7HNb_6O_{19}\cdot 13H_2O$ was prepared according to the literature and its identity was confirmed by IR spectrum.[17] IR spectrum was recorded in the range of 400-4000 cm^{-1} on an Alpha Centaurt FT/IR Spectrophotometer using KBr pellets. Elemental analyses for Cu, V, and Nb were performed with a Leaman

inductively coupled plasma (ICP) spectrometer, and C and N analyses were obtained on a Perkin-Elmer 2400 CHN elemental analyzer. TG analyses were performed on a Perkin-Elmer TGA7 instrument in flowing N_2 with a heating rate of 10 ℃ min^{-1}.

Synthesis of 1. A 2 mL aqueous solution containing 0.040 g $Cu(OAc)_2 \cdot H_2O$ (0.200 mmol) was dropwise added to a 4 mL aqueous solution of $K_7HNb_6O_{19} \cdot 13H_2O$ (0.055 g, 0.040 mmol), As_2O_3 (0.02 g, 0.100mmol) and $NaVO_3$ (0.049 g, 0.400 mmol). Then, 1 ml 1,2-diaminoethane was added dropwise to the mixture. Subsequently, 1 M HCl were used to adjust the pH value of the mixture to 10.50. Then, the mixture was transferred to a Teflon-lined stainless steel autoclave (23 mL) and kept at 160 ℃ for 5 days. When the mixture was slowly cooled to room temperature, brown crystals were obtained and washed with distilled water (yield 40.6 % based on Nb). Elemental analysis calcd (%) for **1**: Cu 10.40, V 11.69, Nb 27.42, C 7.86, N 9.17; Found: Cu 10.62, V 11.32, Nb 27.26, C 7.62, N 9.58.

Synthesis of 2. $K_7HNb_6O_{19} \cdot 13H_2O$ (0.055 g, 0.040 mmol) was added in 4ml aqueous solution of As_2O_3 (0.02 g, 0.100 mmol) and $NaVO_3$ (0.049 g, 0.400 mmol) resulting in solution A. 2 mL aqueous solution containing 0.040 g $Cu(OAc)_2 \cdot H_2O$ (0.200 mmol) was dropwise added to solution A. Then, 1 ml 1,2-diaminoethane was added dropwise to the mixture. The pH value of the mixture was adjusted to 10.80 with 1 M HCl solution, and it was then transferred to a Teflon-lined stainless steel autoclave (23 mL) and kept at 160 ℃ for 5 days. When the mixture was slowly cooled to room temperature, brown crystals were obtained and washed with distilled water (yield 38.2% based on Nb). Elemental analysis calcd (%) for **2**: Cu 10.35, V 13.31, Nb 24.27,

C 7.83, N 9.13; found: Cu 10.56, V 13.82, Nb 24.49, C 7.26, N 9.39.

X-ray crystallography

Single crystals of compounds **1** and **2** were glued onto top of the glass fiber. Data was collected on a Rigaku R-AXIS RAPID IP diffractometer at 293 K using graphite monochromated Mo K_α radiation (λ = 0.71073 Å) and IP techniques. The structures of compounds **1** and **2** were both solved by direct methods and refined by full-matrix least-squares methods on F^2 using the *SHELXTL-97* crystallographic software package.[18] The hydrogen atoms attached to organic ligands were fixed in calculated positions. Further details of the X-ray structural analysis are given in Table 1. Crystallographic data have been deposited with the Cambridge Crystallography Data Centre (CCDC) as deposition numbers CCDC 1047305 and 1047306 for **1** and **2**, respectively. The data can be obtained free of charge from the CCDC, 12 Union Road, Cambridge CB2 1EZ, UK via fax (+44 1223 336033) or e-mail (deposit@ccdc.cam.ac.uk).

Photocatalytic experiments. Photocatalytic performance of compounds **1** and **2** were investigated with photodegradation of RhB and MB solution. 10 mg **1** or **2** were added to 100 mL of 10.0 mg L^{-1} RhB or MB solution. The obtained suspensions were magnetically stirred in the dark for about 30 min to ensure the equilibrium of the working solution. The solution was then exposed to UV irradiation from a 125 W Hg lamp with a distance of 3-5 cm between the liquid surface and the lamp, kept stirring during irradiations.

Results and discussion

Synthesis

During the past decades, hydrothermal synthesis has been proven to be a useful synthetic technique in the preparation of novel POM-based materials. In a specific hydrothermal process, many factors can affect the formation and growth of crystalline products, such as the initial concentration of reactants, pH value, reaction time and temperature. Compound **1** was prepared by the hydrothermal reaction of $K_7HNb_6O_{19}\cdot 13H_2O$, $Cu(Ac)_2\cdot H_2O$, Na_2VO_3, As_2O_3, and en. Parallel experiments showed that the pH value of the reaction system play a significant role in the formation of compound **1**, and the optimized pH value should be in the range from 10.3 to 10.6. It is difficult to prepare compound **1** with a lower pH value than 10.3. Compound **2** was prepared by the similar synthetic procedure with that of **1** except that the pH value of the reaction system of **2** should be in the range of 10.7 to 11.0.

Crystal structure

Compound $[Cu(en)_2(H_2O)][Cu(en)_2]_4\{AsNb_9V_7O_{44}\}\cdot 8H_2O$ (**1**) is composed of an isolated $\{AsNb_9V_7\}$ cluster, decorated by five $[Cu(en)_2]^{2+}$, and charge-balanced by one $[Cu(en)_2]^{2+}$ group. As shown in Route I in scheme 1, the $\{AsNb_9V_7\}$ cluster in compound **1** was composed of a $\{AsNb_8\}$ unit, which captured a $\{NbV_7\}$ ring into the tetravacant PON $[AsNb_8]$ resulted in the anion $[AsNb_9V_7]$. Alternatively, the tetravacant building block $[AsNb_8]$ has sixteen activated oxygen atoms, which could further coordinate with other metal cations. As shown in scheme 1 (Route II), the $[AsNb_8]$ unit captured one $\{NbO_6\}$ and three $\{VO_6\}$ units into a Keggin-type $\{AsNb_9V_3\}$ PON. The Keggin polyoxoanion was then capped by four VO_5 units

resulting in a tetra-capped Keggin-type HPN $\{AsNb_9V_7\}$. Further, the $\{AsNb_9V_7\}$ modified by one $[Cu(en)_2(H_2O)]^{2+}$ and two $[Cu(en)_2]^{2+}$ groups *via* the Cu-O-V/Nb bonds (Fig. 1a). And, the $\{AsNb_9V_7\}$ anion was connected by two $[Cu(en)_2]^{2+}$ into a one-dimensional chain through V-O-Cu bonds, and the V-O and Cu-O distances are in the range of 1.618(9)-1.620(9) Å and 2.537-2.751 Å, respectively (Fig. 1c).

Crystal structure analysis reveals that compound $[Cu(en)_2(H_2O)][Cu(en)_2]_4H\{AsNb_8V_8O_{44}\}\cdot 11H_2O$ (**2**) consists of a $\{AsNb_8V_8\}$ cluster decorated by three $[Cu(en)_2]^{2+}$ groups and charge-balanced by one $[Cu(en)_2(H_2O)]^{2+}$ unit. In compound **2**, the polyoxoanion $\{AsNb_8V_8\}$ is a $\{V_8\}$-cluster-containing HPN. As shown in Fig. 2, the $\{AsNb_8V_8\}$ can be described as a $\{AsV_8\}$ cluster coordinated by two $\{Nb_4O_{18}\}$ units. The $\{AsV_8\}$ cluster is composed of two kinds of VO_x (x = 5 or 6) polyhedra around one AsO_4 tetrahedron. Bond valence calculations indicated that the V centers both in the VO_5 and VO_6 groups are in the IV valence, and the V-O lengths the VO_5 and VO_6 groups are in the range of 1.617(9)-1.960(11)Å and 1.633(8)-2.461(14)Å, respectively (Table S2). The $\{Nb_4O_{18}\}$ fragment is a dimmer consisting of two $[Nb_2O_{10}]^{10-}$ units obtained by decomposition of the Lindqvist cluster $[Nb_6O_{19}]^{8-}$. Two $\{Nb_4O_{18}\}$ moieties capped on the $\{AsV_8\}$ cluster to give the $\{AsNb_8V_8\}$ anion cluster (Fig. 2c), which has been observed in the V- and P-centered PONs.[16a] However, it was first observed in the arsenicniobate compounds. Further, the $\{AsNb_8V_8\}$ cluster was connected by $[Cu(en)_2]^{2+}$ groups into a two-dimensional (2D) porous network through V-O-Cu bonds, and the V-O and Cu-O distances are in the range of 1.633(8)-1.644(9) Å and 2.473-2.523 Å, respectively. As shown in Fig. 4d,

each $\{AsNb_8V_8\}$ cluster was connected with four neighboring polyoxoanions by $[Cu(en)_2]^{2+}$ linkers, resulting in a (4,4)-connected 2D framework with 14.16 × 14.26 Å holes. The 2D frameworks were connected with each other by Cu-O-Nb weak interactions to 3D framework with the Cu-O lengths of 2.929 Å and Nb-O lengths of 1.732(10) Å. In the 3D framework, there are one dimensional channels with the size of 7.5 Å × 7.2 Å along the b-axis (Fig. 3). The $[Cu(en)_2(H_2O)]^{2+}$ groups are located in the channels of the 3D framework, balancing the charge of the framework.

Thermal analyses

To study the thermal stability of compounds **1** and **2**, the thermogravimetric (TG) analysis was carried out on these two compounds. As shown in Fig. S3, the TG curve of compound **1** shows three step weight losses in the range of 50 to 600 ℃. The first weight loss of 5.54% occurs between 50 and 200 ℃, corresponding to the loss of lattice water molecules (cal. 5.31%). The other two weight loss of 9.91% is from 200 to 400 ℃ and 6.86% from 400 to 600 ℃, corresponding to the loss of the ligands in the 1D framework (cal. 19.66%). The TG curve of compound **2** shows a weight loss of 6.20% between 50 and 200 ℃ (Fig. S4), corresponding to the loss of lattice water molecules (cal. 7.05%). The other two weight loss of 9.7% is from 200 to 400 ℃ and 8.06% from 400 to 600 ℃, corresponding to the loss of the ligands in the 3D framework (cal. 19.57%).

IR spectra

The IR spectrum of compounds **1** and **2** display similar characteristic vibration patterns, resulting from the HPONs in the region of 400-1100 cm^{-1}, is shown in Fig.

S5 and S6. The terminal M = Ot (M = V and Nb) vibrations appear at 953 and 893, 807 cm^{-1} for **1**, 951, 895, and 811 cm^{-1} for **2**, respectively.[10,16] The characteristic peaks at 648, 604, 490 cm^{-1} for **1**, 649, 604, and 477 cm^{-1} for **2** are assigned to the bridging M-O_b-M vibrations, respectively. Bands at 1040 cm^{-1} are assigned to As-O_c vibration of **1** and **2**.[10,16] The characteristic absorption bands of the organic groups appear at 1102-1585 cm^{-1} and 1098-1583 cm^{-1} for **1** and **2**, respectively.

Photocatalytic property

In the past decades, photocatalysts have been widely studied to decompose waste organic dyes so as to purify water resources. Methylene blue (MB) and rhodamine B (RhB) are typical dye molecules to evaluate the activity of photocatalysts used for the purification of waste water.[19-21] POMs have regarded as one type of new potential photocatalysts in the degradations of organic dyes.[20] However, POM salts are usually water-soluble and may induce secondary pollution if they are directly used as photocatalysts in aqueous solution, and they are difficult to be isolated for reuse. Up to date, much attention has been paid to the construction of novel heterogeneous POM-based photocatalysts.[20] Herein, the heterogeneous photocatalytic performance of compounds **1** and **2** towards degradation of MB and RhB under UV irradiation were investigated. In the presence of compound **1**, the MB and RhB degrades from 100% to 6.3% and 19.8% during 2.5 h, the degradation rate curve of **1** is nearly linear, corresponding to about 37.5% and 32.1% per hour (Fig. 4a, 4b). For compound **2**, MB and RhB degrades to 7.8% and 11.8% during 2.5 h and the degradation rate is 36.9% and 35.3% per hour (Fig. 4c, 4d). A control photolysis experiment was also performed

under the same conditions by using $Cu(en)_2$ as the catalyst or without any catalyst. After 2.5h photocatalytic process, the decolorization rate of MB solution can only achieve 9.8% and 4.5%, respectively, and the decolorization rate of RhB solution can achieve 6.0% and 3.9%, respectively (Fig. S7). These results reveals that compounds **1** and **2** are active photocatalysts for the degradation of MB and RhB. As shown in Fig. S8 and S9, the PXRD pattern of as-synthesized samples is in good agreement with that of the simulated one from the single crystal data, which proves the phase purity of the bulk materials. Further, the PXRD pattern of the photocatalyst after the photocatalytic reaction also shows similar peaks with that of the as synthesized sample, revealing that the photocatalyst is stable in the photocatalytic reaction. Additionally, we found that the catalytic activity of compounds **1** and **2** was maintained in the recycled experiments, no significant loss in photocatalytic activity was observed (Fig. S10, S11).

Conclusion

In conclusion, we reported two extended structures based on transition-metal-cluster-substituted arsenicniobate clusters. Compounds **1** and **2** contain a similar travacant PON $[AsNb_8O_{36}]^{27-}$ clusters, which captured the $\{V_8\}$ and $\{NbV_7\}$ rings forming the transition-metal-cluster-substituted polyoxoarsenicniobates. In this work, the As atom was introduced into the hereropolyoxoniobate system, which indicated a promising filed for constructing new PON-based materials. Photocatalytic studies revealed that compounds **1** and **2** are active for photocatalytic degradation of dye molecules.

Acknowledgments

This work was supported by the National Natural Science Foundation of China (21101022), and Science and Technology Development Project Foundation of Jilin Province (20150520001JH).

References

(1) (a) A. Müller, F. Peters, M. T. Pope, D. Gatteschi, *Chem. Rev.*, 1998, **98**, 239-271; (b) D. L. Long, R. Tsunashima, L. Cronin, *Angew. Chem. Int. Ed.*, 2010, **49**, 1736-1758; (c) S. T. Zheng, G. Y. Yang, *Chem. Soc. Rev.*, 2012, **41**, 7623-7646.

(2) (a) A. Dolbecq, E. Dumas, C. R. Mayer, P. ialane, *Chem. Rev.*, 2010, **110**, 6009-6048; (b) H. J. Lv, Y. V. Geletii, C. C. Zhao, J. W. Vickers, G. B. Zhu, Z. Luo, J. Song, T. Q. Lian, D. G. Musaev, C. L. Hill, *Chem. Soc. Rev.*, 2012, **41**, 7572-7589.

(3) (a) Q. X. Han, C. He, M. Zhao, B. Qi, J. Y. Niu, C. Y. Duan, *J. Am. Chem. Soc.*, 2013, **135**, 10186-10189; (b) X. B. Han, Z. M. Zhang, T. Zhang, Y. G. Li, W. Lin, W. You, Z. M. Su, E. B Wang, *J. Am. Chem. Soc.*, 2014, **136**, 5359-5366; (c) Z.-M. Zhang, T. Zhang, C. Wang, Z. Lin, L.-S. Long, W. Lin, *J. Am. Chem. Soc.*, 2015, 137, 3197−3200.

(4) (a) M. Nyman, *Dalton Trans.*, 2011, **40**, 8049-8058; (b) J. Y. Niu, F. Li, J. W. Zhao, P. T. Ma, D. D. Zhang, B. Bassil, U. Kortz, J. P. Wang, *Chem. Eur. J.*, 2014, **20**, 9852-9857; (c) R. L. Johnson, E. M. Villa, C. A. Ohlin, J. R. Rustad, W. H. Casey, *Chem. Eur. J.*, 2011, **17**, 9359-9367.

(5) (a) J. Y. Niu, G. Wang, J. W. Zhao, Y. X. Sui, P. T. Ma, J. P. Wang, *Cryst. Growth Des.*, 2011, **11**, 1253-1261; (b) J. Y. Niu, G. Chen, J. W. Zhao, P. T. Ma, S. Z. Li, J. P. Wang, M. X. Li, Y. Bai, B. S. Ji, *Chem. Eur. J.*, 2010, **16**, 7082-7086; (c) M. Maekawa, Y. Ozawa, A. Yagasaki, *Inorg. Chem.*, 2006, **45**, 9608-9609.

(6) (a) R. Tsunashima, D. L. Long, H. N. Miras, D. Gabb, C. P. Pradeep, L. Cronin,

Angew. Chem. Int. Ed., 2010, **49**, 113-116; (b) R. P. Bontchev, M. Nyman, *Angew. Chem. Int. Ed.*, 2006, **45**, 6670-6672.

(7) (a) C. A. Ohlin, E. M. Villa, J. C. Fettinger, W. H. Casey, A*ngew. Chem. Int. Ed.*, 2008, **47**, 5634-5636; (b) G. L. Guo, Y. Q. Xu, J. Cao, C. W. Hu, *Chem. Eur. J.*, 2012, **18**, 3493-3497.

(8) M. Nyman, F. Bonhomme, T. M. Alam, M. A. Rodriguez, B. R. Cherry, J. L. Krumhansl, T. M. Nenoff, A. M. Sattler, *Science*, 2002, **297**, 996-998.

(9) (a) Y. Hou, T. M. Alam, M. A. Rodriguez, M. Nyman, *Chem. Commun.*, 2012, **48**, 6004-6006; (b) M. Nyman, J. P. Larentzos, E. J. Maginn, M. E. Welk, D. Ingersoll, H. Park, J. B. Parise, I. Bull, F. Bonhomme, *Inorg. Chem.*, 2007, **46**, 2067-2079; (c) Z. Y. Zhang, Q. P. Lin, D. Kurunthu, T. Wu, F. Zuo, S. T. Zheng, C. J. Bardeen, X. H. Bu, P. Y. Feng, *J. Am. Chem. Soc.*, 2011, **133**, 6934-6937.

(10) (a) M. Nyman, F. Bonhomme, T. M. Alam, J. B. Parise, G. M. B. Vaughan, *Angew. Chem. Int. Ed.*, 2004, **43**, 2787-2792; (b) G. L. Guo, Y. Q. Xu, J. Cao, C. W. Hu, *Chem. Commun.*, 2011, **47**, 9411-9413.

(11) (a) B. Nohra, H. E. Moll, L. M. R. Albelo, P. Mialane, J. Marrot, C. Mellot-Draznieks, M. O'Keeffe, R. N. Biboum, J. Lemaire, B. Keita, L. Nadjo, A. Dolbecq, *J. Am. Chem. Soc.*, 2011, **133**, 13363-13374; (b) Q. Lan, J. Zhang, Z. M. Zhang, Y. Lu, E. B. Wang, *Dalton Trans.*, 2013, **42**, 16602-16607; (c) J. Lü, J. X. Lin, X. L. Zhao, R. Cao, *Chem. Commun.*, 2012, **48**, 669-671.

(12) (a) S. B. Li, H. Y. Ma, H. J. Pang, L. Zhang, *Cryst. Growth Des.*, 2014, **14**, 4450-4460; (b) R. Li, X. Q. Ren, J. S. Zhao, X. Feng, X. Jiang, X. X. Fan, Z. G.

Lin, X. G. Li, C. W. Hu, B. Wang, *J. Mater. Chem. A*, 2014, **2**, 2168-2173; (c) A. X. Yan, S. Yao, Y. G. Li, Z. M. Zhang, Y. Lu, W. L. Chen, E. B. Wang, *Chem. Eur. J.*, 2014, **20**, 6927-6933; (d) B. F. Chen, F. B. Li, Z. J. Huang, T. Lu, Y. Yuan, J. L. Yu, G. Q. Yuan, *RSC Adv.*, 2012, **2**, 11449-11456.

(13) J. Rabeah, A. Dimitrov, A. Surkus, H. Jiao, W. Baumann, R. Stößer, J. Radnik, U. Bentrup, A. Brückner, *Organometallics*, 2014, **33**, 4905-4910.

(14) (a) Q. H. Geng, Q. S. Liu, P. T. Ma, J. P. Wang, J. Y. Niu, *Dalton Trans.*, 2014, **43**, 9843-9846; (b) S. J. Li, S. X. Liu, C. C. Li, F. J. Ma, W. Zhang, D. D. Liang, R. K. Tan, Y. Y. Zhang, Q. Tang *Inorg. Chim. Acta*, 2011, **376**, 296-301.

(15) Z. Y. Zhang, J. Peng, Z. Y. Shi, W. L. Zhou, S. U. Khana, H. S. Liu, *Chem. Commun.*, 2015, **51**, 3091-3093.

(16) (a) J. Q. Shen, Q. Wu, Y. Zhang, Z. M. Zhang, Y. G. Li, Y. Lu, E. B. Wang, *Chem. Eur. J.*, 2014, **20**, 2840-2848; (b) J. Q. Shen, Y. Zhang, Z. M. Zhang, Y. G. Li, Y. Q. Gao, E. B. Wang, *Chem. Commun.*, 2014, **50**, 6017-6019; (c) Y. Zhang, J. Q. Shen, L. H. Zheng, Z. M. Zhang, Y. X. Li, E. B. Wang, *Cryst. Growth Des.*, 2014, **14**, 110-116.

(17) M. Filowitz, R. K. C. Ho, W. G. Klemperer, W. Shum, *Inorg. Chem.*, 1979, **18**, 93-103.

(18) (a) G. M. Sheldrick, SHELXL97, Program for Crystal Structure Refinement, University of Göttingen, Göttingen, Germany, 1997. (b) G. M. Sheldrick, SHELXS97, Program for Crystal Structure Solution, University of Göttingen, Göttingen, Germany, 1997.

(19)(a) C. C. Chen, W. Zhao, P. X. Lei, J. C. Zhao, N. Serpone, *Chem. Eur. J.*, 2004, **10**, 1956-1965; (b) X. L. Wang, J. Li, A. X. Tian, D. Zhao, G. C. Liu, H. Y. Lin, *Cryst. Growth Des.*, 2011, **11**, 3456-3462; (c) A. X. Tian, X. L. Lin, X. J. Liu, J. Ying, X. L. Wang, *RSC Adv.*, 2013, **3**, 17188–17194.

(20)(a) A. Dolbecq, P. Mialane, B. Keita, L. Nadjo, *J. Mater. Chem.*, 2012, **22**, 24509-24521; (b) Z. J. Liu, S. Yao, Z. M. Zhang, E. B. Wang, *RSC Adv.*, 2013, **3**, 20829-20835; (c) Q. Lan, Z. M. Zhang, Y. G. Li, Y. Lu, E. B. Wang, *Dalton Trans.*,2014, **43**, 16265-16269.

Table 1 Crystal data and structure refinement for **1** and **2**.

	1	**2**
Empirical formula	$C_{20}H_{98}N_{20}O_{53}AsNb_9V_7Cu_5$	$C_{20}H_{105}N_{20}O_{56}AsNb_8V_8Cu_5$
*F*w	3052.5	3065.5
Crystal system	Monoclinic	Triclinic
Space group	$C_{2/c}$	P_{-1}
a (Å)	25.852(5)	12.907(3)
b (Å)	27.121(5)	14.153(3)
c (Å)	24.729(5)	14.277(3)
β (°)	109.49(3)	80.34(3)
V (Å^3)	16345(6)	2300.9(8)
Z	8.00	1.00
T (K)	293(2)	293(2)
λ (Å)	0.71073	0.71073
R_1, wR_2 [$I>2\sigma(I)$]	0.0707, 0.1748	0.0826, 0.2230
R_1, wR_2 (all data)	0.1058, 0.1932	0.1012, 0.2378

Note. $R_1 = \Sigma||F_o|-|F_c||/\Sigma|F_o|$; $wR_2 = \Sigma[w(F_o^2-F_c^2)^2]/\Sigma[w(F_o^2)^2]^{1/2}$.

Fig. Captions

Scheme 1. Schematic view of the polyoxoanion structure in **1**.

Fig. 1. (a) Ball-and-stick view of the structural unit of **1**; (b) Polyhedral representation of the $\{V_8\}$ cluster in **2**; (c) Structure of the 1D chain composed of the $\{AsNb_9V_7\}$ units and $[Cu(en)_2]^{2+}$ groups in **1**.

Fig. 2. (a) Ball-and-stick representation of the $\{Nb_4\}$ unit both in **1** and **2**; (b) polyhedral representation of the $\{AsV_8\}$ unit in **2**; (c) polyoxoanion $\{AsNb_8V_8\}$ consists of a $\{AsV_8\}$ cluster and two $\{Nb_4\}$ units in **2**; (d) 2D framework of **2** constructed from the polyoxoanion $\{AsNb_8V_8\}$ and $[Cu(en)_2]^{2+}$ groups.

Fig. 3. 3D porous framework of **2** along the *b*-axis.

Fig. 4. Photocatalytic degradation of MB (a) and RhB (b) by compound **1**; Photocatalytic degradation of MB (c) and RhB (d) by compound **2**.

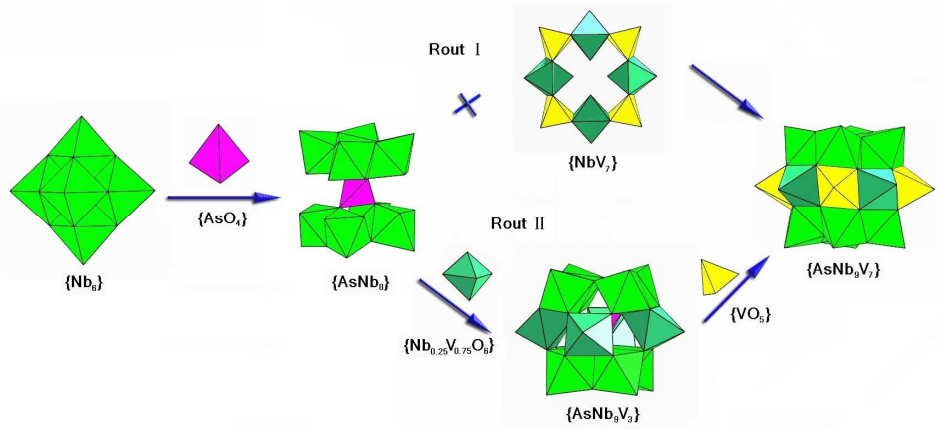

Scheme 1

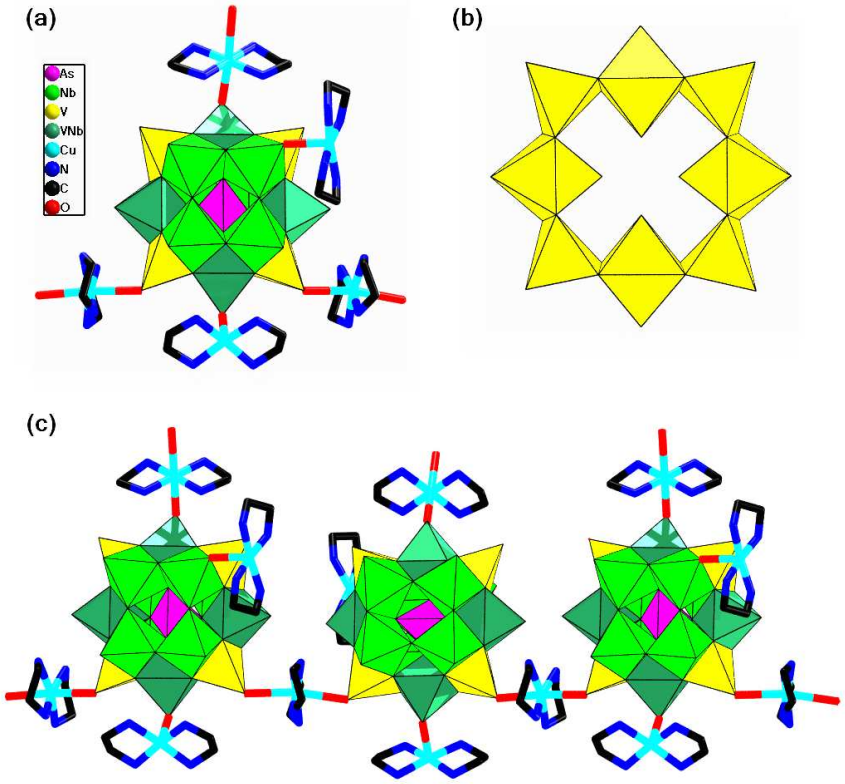

Fig. 1

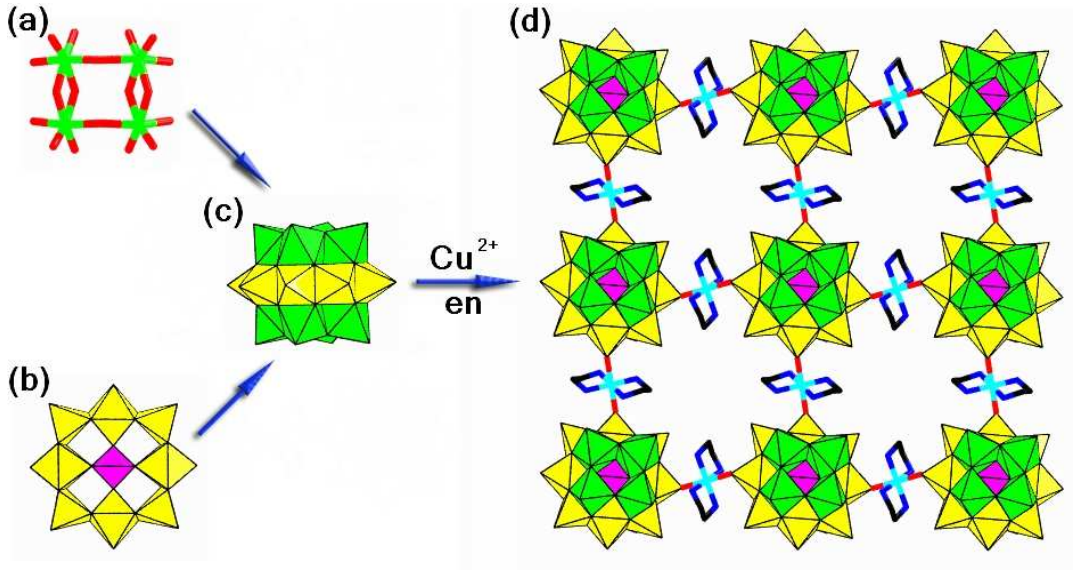

Fig. 2

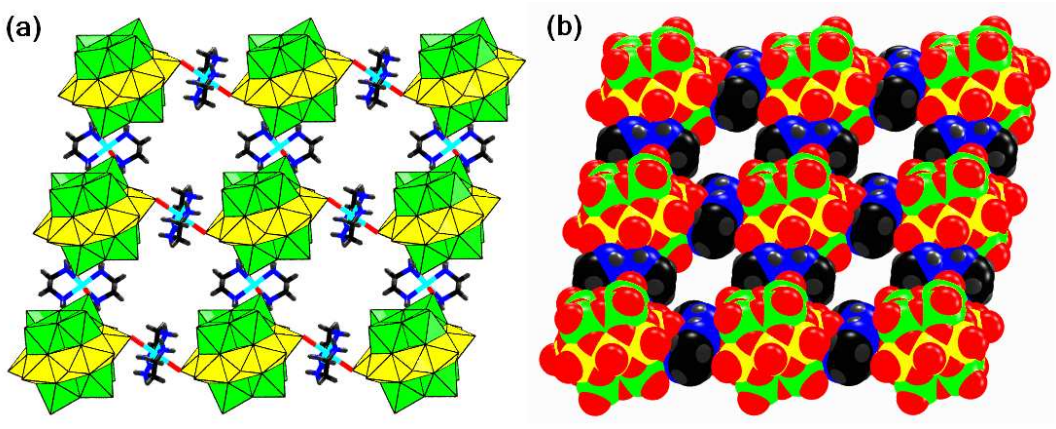

Fig. 3

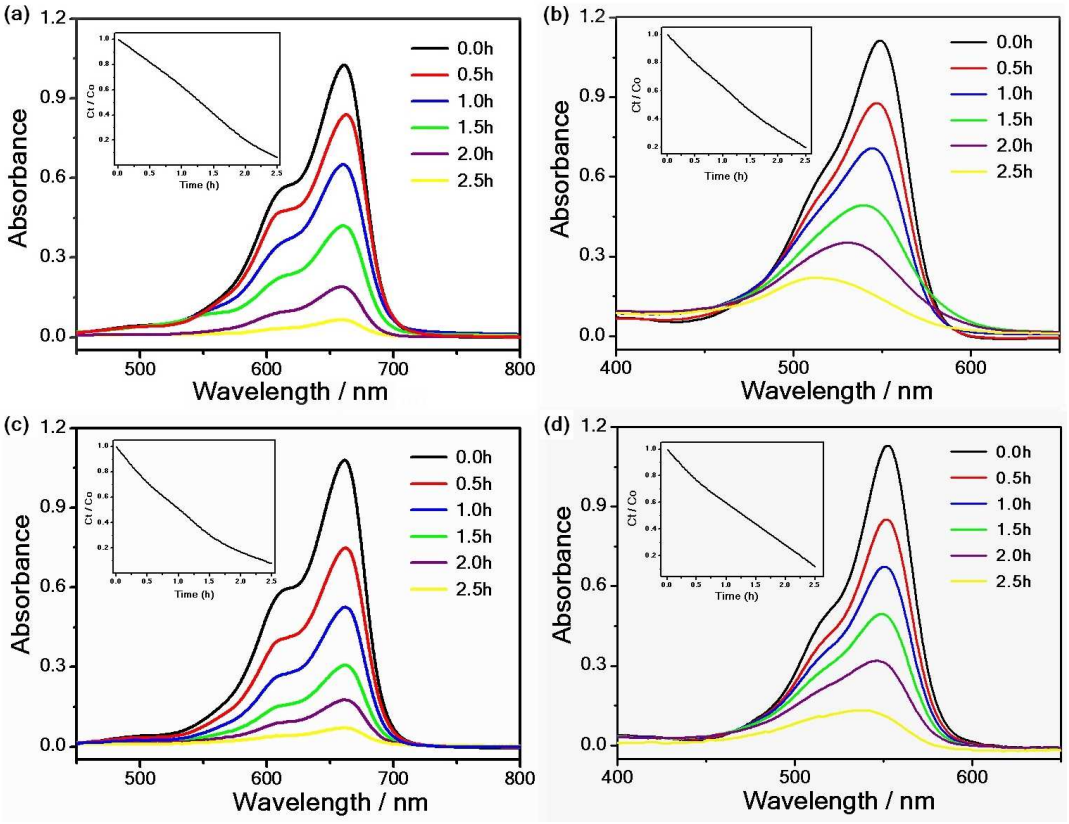

Fig. 4